Erschienen in: Computational Materials Science ; 183 (2020). - 109886
https://dx.doi.org/10.1016/j.commatsci.2020.109886

Automatic Etch Pit Density Analysis in Multicrystalline Silicon

Martin Fleck, Giso Hahn
Universität Konstanz

Abstract

This publication contains a description and is published in combination with the source code for a tool capable of determining the etch pit density (EPD) on multicrystalline silicon image data. The algorithm is capable of classifying grain boundaries and polishing scratches and removes these structures from the analysis result. Included with the analysis code are methods for plotting EPD maps as well as relative EPD frequency. This is combined with a brief description of the experimental steps of wafer preparation and defect etching as well as a discussion of the analysis limitations.
Keywords: Defect etching, Etch Pit Density, dislocation density, crystal defects, multicrystalline silicon, mc-Si

1. Introduction

Publications concerned with etch pit density (EPD) measurements in multicrystalline Silicon (mc-Si) material often estimate the EPD based on flatbed scanning images [1] [2] [3] or use indirect measurements of the EPD [4]. Optical microscope images, with sufficient precision to directly observe etch pits and therefore directly measure the EPD are normally used as reference images for very small regions only [2]. In this paper an algorithm is presented that allows to combine the precision of optical microscope images sufficient for counting individual etch pits with analysis of large wafer areas of several cm^2. This technique has been successfully applied for detection and investigation of changes in etch pit density due to gettering steps [5]. In the following it is explained how wafers are prepared, defect etching is executed and how optical microscope data is reduced to EPD values.

2. Sample preparation for defect etching

For computer aided etch pit counting that is capable of detecting individual etch pits, it is crucial that prior to defect etching, the wafer surface appears featureless when analysed with the optical microscope. Wafer surfaces after chemical polishing retain some surface roughness, resulting in surface structures that exhibit comparable contrast to etch pits when analysed with the optical

microscope. Therefore chemically polished material has been found unsuited for computer aided EPD analysis in our study. Best results have been achieved with chemo-mechanical polishing of individual samples that result in surfaces that appear perfectly smooth on magnification scales used in the optical microscope. Results presented in this work are based on Secco [6] etches of chemo-mechanically polished wafer surfaces. The Schimmel etch [7] and the Sopori etch [8] have been used successfully as well. The Wright etch [9] has been found to attack the polished surface in some grains and therefore was found unsuitable for EPD analysis on mc-Si material in our study.

Samples are cut with laser to a size of 25 mm × 12 mm. Samples of this size are polished with a Logitech PM5 Polishing System and a Logitech PP6 jig, using a polishing table of 300 mm diameter that is operated at 20 rotations/min and using 33 kPa sample pressure. Polishing is a two-step process: First, the sample surface is flattened, using the finest grain paper that is capable of removing material sufficiently quick such that a flat surface is reached in a couple of minutes. Sand papers with grain sizes of 10 µm and some sand papers with a grain size 5 µm have been found suitable for this task. The second, final step is done using an alkaline colloid solution of SiO_2 of 0.032 µm grain size (LOGITECH Syton Typ SF1) on an aluminium-oxide foam plate. All parts that are in contact with the polishing surface should be thoroughly rinsed and cleaned with a piece of cloth when switching to the finer polishing step. Polishing with the SF1 solution results in a homogeneous, mirror-like surface. A challenging problem is that a surface that seems perfectly devoid of scratches and marks under the optical microscope can still reveal scratches after the defect etching process. Typically, 90 min of SF1 polishing results in a surface that is free of scratches after defect etching.

We use two 10 min cascades of piranha solution, a mixture of three parts H_2SO_4 (30 %) and one part H_2O_2 (95 % to 97 %), for removing the glue that is used to attach the sample to the jig. Subsequent dipping of the samples in diluted HF immediately before the defect etch step reduces dissimilarities in etching results between wafers.

3. The defect etch process with the Secco etch

On boron doped, industry standard mc-Si material with a resistivity of 1 Ωcm, a 90 s ultrasonically agitated Secco etch has been found suitable for delineation of defects that are reliably detectable in the optical microscope at 50x total magnification (5x magnifying lens, 10x magnifying eyepiece/camera). Furthermore, it has been found that etch times of at least 60 s are required such that all etch pits are etched to sufficient size for reliable detection. Larger etching times can be beneficial, when the algorithmic grain boundary removal is failing. However, larger etching times reduce the data quality in regions of high etch pit density.

4. Optical microscope data taking

Images should be exposed such that the contrast between etch pits and wafer surface is maximized. Ideally, the exposure is chosen such that an etch pit retains a few perfectly black pixels (RGB 0,0,0) with the background as bright as possible. A slight overexposure of the background is acceptable, as long as etch pits are still black. Microscope images of the wafer surface are stitched to a single composite image. If possible, the vignetting of the microscope optics should be removed from the recorded images before image stitching.

5. Computer aided etch pit density analysis

5.1. Overview

Distinguishing between interesting structures on the wafer and the wafer surface (background) relies on contrast between background and structures of interest. Separation is achieved by converting the gray scale microscope image to binary image data using a threshold value: A pixel with a gray scale value below the threshold value is stored as 0, all pixels above the threshold are stored as 1. Resulting regions of connected ones or zeros are analysed with the *regionprops* algorithm that has implementations e.g. in the Python package *scikit-image* Matlab. Executing *regionprops* on a binary image containing connected structures generates a list-like object that for each structure contains a set of properties, such as a structure's center of mass coordinate or its size in pixels, etc. This principle of etch pit detection via thresholding and analysis has been presented by Needleman et al. [3].

Etch pits occur in one of three categories : 1. Isolated (single) etch pits 2. A group of overlapping etch pits that is small compared to the size of a single pixel in the final EPD map. These etch pit conglomerates are typically found in mid-EPD regions 3. Regions where etch pits are so dense that they cluster together to a single structure (etch pit clusters). Etch pit clusters differ from conglomerate structures in so far that they are larger than a pixel of the final EPD map. A distinction between these three cases (figure 1) has to be made. Structures belonging to case 2 consist of multiple etch pits. A good estimator for the number of etch pits that make up a conglomerate structure can be obtained by dividing its size by the size of a typical etch pit. For case 3, further steps are necessary because etch pit clusters are typically much larger than a single image pixel in the resulting EPD map, therefore the shape of the etch pit cluster has to be considered. Additionally, etch pit clusters are often connected to grain boundaries, hence a distinction between grain boundaries and etch pit clusters has to be made. After separation of grain boundaries and etch pit clusters, cluster EPD has to be estimated. Subsequently, the location information of etch

pits withing the cluster is obtained by uniformly distributing etch pits onto the cluster area until the estimated EPD is reached. Finally, location information (x,y) of etch pits of all three cases are saved, from which an EPD map can be inferred. The following details the procedures of these steps.

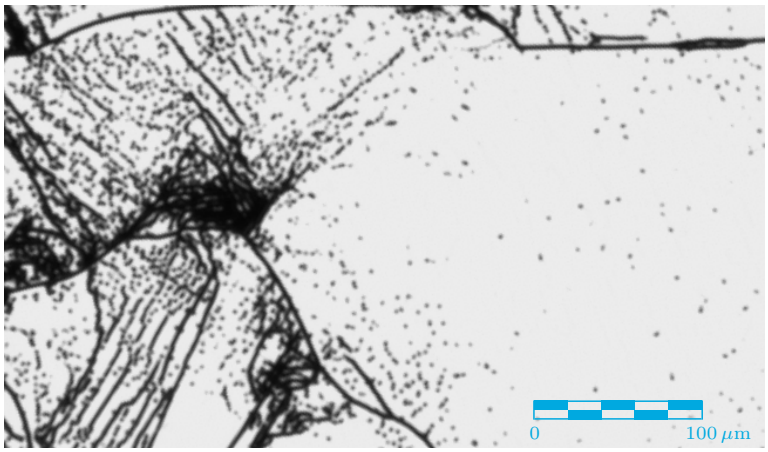

Figure 1: Optical microscope image of a typical mc-Si wafer after defect etching, showing clustered regions of high EPD, next to regions of mid and low EPD. Low EPD regions feature individual etch pits (e.g. bottom right), isolated structures in regions of medium EPD often correspond to conglomerates of multiple etch pits (e.g. top left), which are identified by size and weighted according to their relative area during etch pit counting. It is clear that for etch pit clusters, as seen in the left center, counting of individual etch pits is not possible. A lower limit for the EPD in clusters can be estimated based on the cluster area and the median area of isolated etch pits, as is described in the text.

5.2. Preparation

A few manual steps are required before the algorithm can be run. First, images are cropped, such that only the wafer surface is part of the image. If parts of the image are not suited for analysis, e.g. due to heavily scratching or surface stains, these regions are deleted from the image. Heavily scratched areas typically are found in the sample's corners.

Finally, a suitable threshold value must be determined. A typical image editor such as GIMP can be used to apply the threshold function and visually compare the structures in the resulting binary image with the etch pits seen in the original image. As many etch pits as possible should have a corresponding structure in the binary image whereas no noise (single pixels that exceed the threshold) from the background should appear. Typically, most parts of the wafer can be exposed such that there is clear contrast between etched structures and the wafer surface. In these cases there is a wide range of threshold values available that can be used with good results. Certain grains occasionally develop a less reflective surface after defect etching such that the wafer surface appears darker. Especially in these dark grains, threshold values should be crosschecked for the appearance of noise.

5.3. Description of the algorithm

Images prepared in this way are fed to the algorithm and converted to a binary image using the previously determined threshold value. Next, a distinction between large and small structures is made: two new binary images are created, one of which contains only structures below a certain size S and the other image containing all structures above the size S (figure 2). The resulting EPD map does not sensitively depend on S since for both, large and small structures, there is a check whether they consist of multiple etch pits. For etch pits of large structures, individual spatial coordinates are attributed, ensuring that etch pits from a large structure can contribute to multiple different pixels of the resulting EPD map. Therefore, S should be chosen smaller than the area of EPD image pixels. Structures with sizes smaller than S are either individual etch pits, specs of noise (i.e. single pixels that exceed the threshold value) or etch pit conglomerates of a few etch pits, typically appearing in mid-EPD regions (figure 1). A distinction between these three cases can be made based on structure size and happens at a later stage. Structures larger than S can be surface stains or, more importantly, grain boundaries and clusters of etch pits (figure 1).

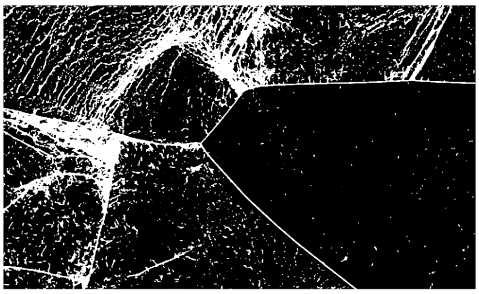

(a) Binary image

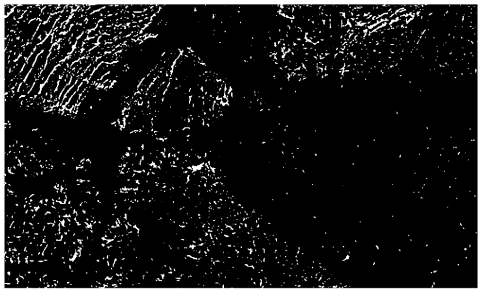

(b) Small structures

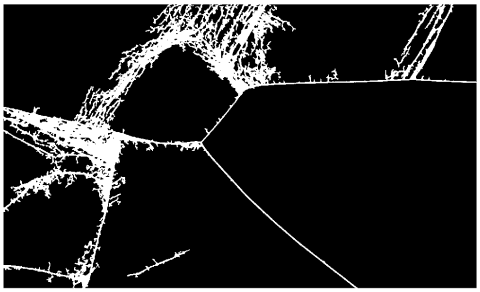

(c) Large structures

Figure 2: The input binary image (a) is split into two images, one containing only small structures with size below S (b), the other containing the remaining large structures (c). The wafer section shown here is about 1 mm wide and only shows 0.2 % of the wafer surface that is analysed.

The image that contains the small structures only is analysed with *regionprops*. Center of mass location of the regions and their size in pixels are saved as lists. While the analysis of small structures is straightforward, lots of the large structures are grain boundaries, a plane-like defect, that should not contribute to the density of etch pits that are due to line-like (and possibly some surface-close point-like) defects. Grain boundaries and defect clusters are often in direct vicinity and form a single structure in the binary image. In addition, all grain boundaries of a wafer are connected with one another. Again, *regionprops* can potentially be used for distinction between grain boundaries (line structures) and etch pit clusters (cloud like structures, often with holes), however, *regionprops* requires separate, disconnected structures. For this purpose, the image is superimposed with a square grid of white pixels, effectively subdividing large structures into smaller square tiles. The tile size should be small compared to the grain size of the material. This assures that a typical grain boundary fragment within a tile is likely to be a straight line - a property that is used for distinction between grain boundaries and etch pit clusters. On the other hand the tile size must be well above the thickness of etched grain boundary structures after thresholding, such that grain boundary fragments within a tile remain highly elongated structures. These criteria leave a wide range of suitable tile sizes. A tile size of 300 pixels corresponding to 210 µm, or about 30 to 50 times the thickness of a typical grain boundary, is used here. Variations of the tile size only have small effect on the grain boundary removal process as long as they remain within the discussed limits.
After splitting the image into tiles, *regionprops* is used for analysis of each tile's contents: The distinction between grain boundaries and etch pit clusters is made on two criteria: The eccentricity ϵ of an ellipse that has the same normalized second central moments (measures for the regions shape) as the region in question and the region's Euler Number, a measure for the number of holes that a region contains. Regions with $\epsilon > 0.93$, i.e. structures highly elongated in one direction, are classified as grain boundaries. Secondly, regions with three or less holes are classified as grain boundaries. Regions classified as grain boundaries are discarded, the remaining regions are treated as etch pit clusters. With these simple criteria, most grain boundaries, twin grain boundaries and polishing scratches can be removed (figure 3).

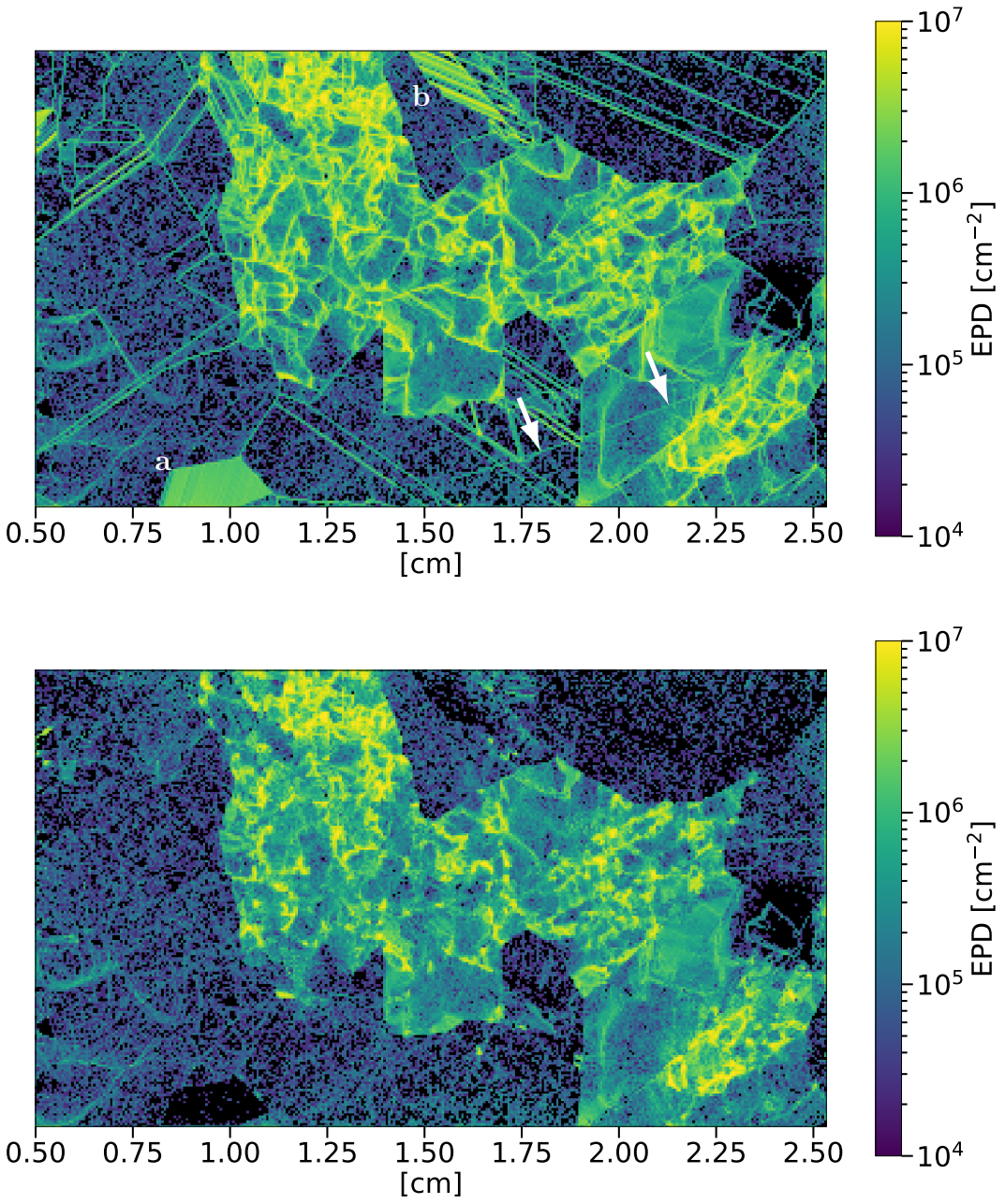

Figure 3: Etch pit density analysis result before (top) and after (bottom) grain boundary removal. Grain regions with twin boundaries (marked "a" and "b") show meaningful values only after grain boundary removal. Polishing scratches (marked with arrows) are removed, too. The shape of etch pit clusters, however, can be influenced by the grain boundary removal process. With grain boundaries removed, only data due to etch pits remains as basis for the image, allowing for a further data reduction step.

The etch pit density in a cluster can be estimated from the cluster's size (the number of pixels

that it contains) and the size (the number of pixels) A of a typical etch pit, using the pixel size of microscope images for conversion . The EPD in clusters estimated in this way constitutes a lower limit to the true value and the EPD value explicitly depends on A. While calculating A for each image separately is easily possible, the A dependant cluster EPD requires a constant value of A when sets of sister wafers are to be compared.

After splitting the large structures into tiles and after sorting grain boundaries from etch pit clusters, the algorithm fills up the area of etch pit clusters with uniformly distributed etch pits until the previously calculated EPD value is reached: For every cluster region, a list-like data object that contains the coordinates of all pixels that make the structure is obtained and reduced such that it contains only every A^{th} entry, with A the number of pixels of a typical etch pit. This reduced pixel list is saved to the output file, providing the location information of etch pits of an etch pit cluster, based on the assumption that the whole cluster area is composed of etch pits of size A. Additionally, meta information about the analysis, such as the input image file's name and path, the used values for threshold, grain boundary detection (eccentricity ϵ, Euler Number and grid tile size), the assumed value for the etch pit size A in clusters and the magnification of the optical microscope setup are saved.

It is important to note that this procedure can only give a lower limit for the true etch pit density in clusters. In etch pit clusters, the distance between two etch pits can become smaller than the radius of a typical etch pit. In these conditions multiple etch pits can overlap with each other and the assumption that the area of an etch pit cluster is proportional to the number of etch pits that are contained in the cluster is systematically underestimating the true EPD in these regions. Scanning electron microscope studies have shown that in highly localized subregions of etch pit clusters, the EPD can exceed the estimated value by up to two orders of magnitude.

Due to the large size of the input images (more than 6×10^8 pixels) the computation of structured etch pit data from the raw image can take up to four minutes on a 2012 i5-3320M mobile CPU, whereas filtering and plotting the structured etch pit data set can be accomplished within a few seconds. The time consuming step of reducing the raw image data to list-like data has therefore been separated from the step of data plotting.

At the plotting stage, etch pit size filtering is applied, i.e. etch pits with a size fewer than 3 pixels are discarded as noise. Unwanted wafer regions, such as missing wafer parts due to breakage or the part of the wafer that has been in contact with the carrier during defect etching, are cropped.
At this stage, etch pit conglomerates, defined as etch pits that have a size $C > 2A$, with A the size of a typical etch pit, are weighted with a factor $\frac{C}{A}$, effectively counting them as multiple etch pits according to their size. Again, keeping A constant is required for a meaningful comparison between

sister wafers.

6. Data visualization

Etch pit data is visualised in the form of a two dimensional histogram, with the vertical and horizontal axes corresponding to the physical dimensions of the wafer and the bin height corresponding to the etch pit density (figure 3). It is noteworthy that the process of binning the data determines a lower limit of the EPD: The minimal (non-zero) EPD value, associated with one etch pit per bin, depends on the bin size. A physically meaningful bin size can be chosen using the minority charge carrier diffusion length as characteristic length scale for the bin width. However, in typical mc-Si material there are regions of very high and low diffusion length in close proximity, so a compromise is necessary. Bins that are too large will hide etch pit structures. If bins are very small (about the size of an etch pit), density calculation becomes meaningless. Larger bin sizes allow for easier interpretation of results in low EPD regions but at the cost of hiding structure in mid and high density regions (figure 4). For plots that are easier to read, empty bins are drawn in black. The analysis contains a simple routine for image cropping, such that the EPD analysis is restricted to a rectangular subregion of the wafer.

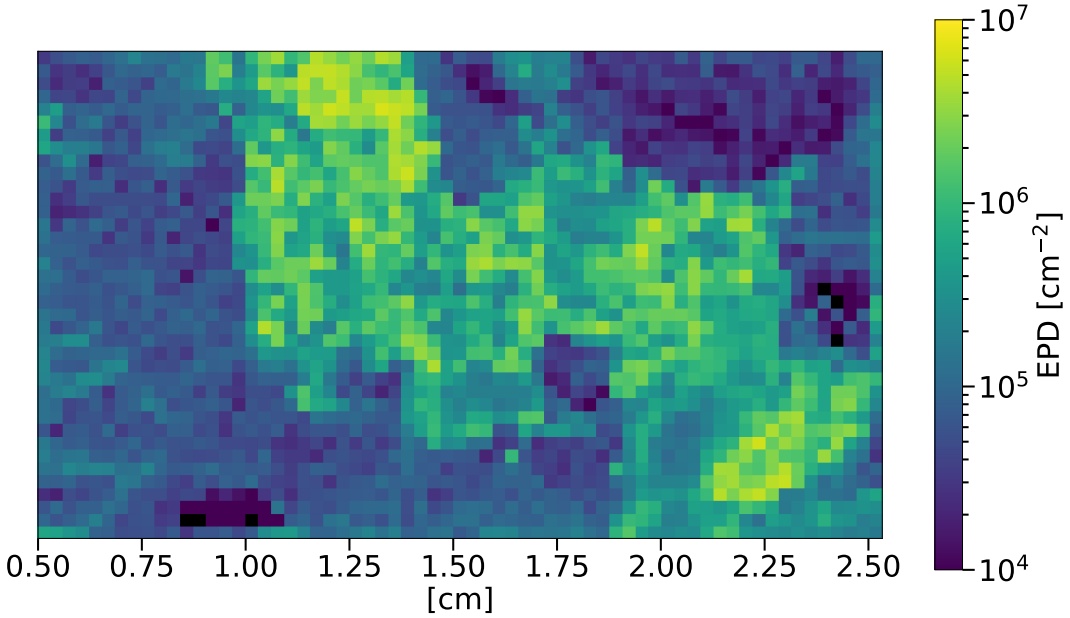

Figure 4: An EPD map of the wafer shown in figure 3 (with grain boundaries removed), here shown with bin width of 300 µm, about five times the bin with that is used in the other EPD maps shown in this work. While low EPD regions within grains are easier resolved, EPD structures in mid and high EPD regions can not be resolved with this bin size.

While spatial maps are good for comparisons with other spatial measurements, possible changes in EPD can be better quantified if the data is further reduced: Therefore, a method to create one dimensional histograms is part of the functionality, with which the fraction of the wafer surface affected by a certain EPD is plotted (figure 5). A distribution of the area fraction as function of EPD allows for a good understanding of a wafer's EPD, while at the same time the comparison between two distributions of this type give a good impression on possible changes in EPD. The ratio between two area fraction histograms makes quantification of EPD changes due to a certain process easier (figure 5).

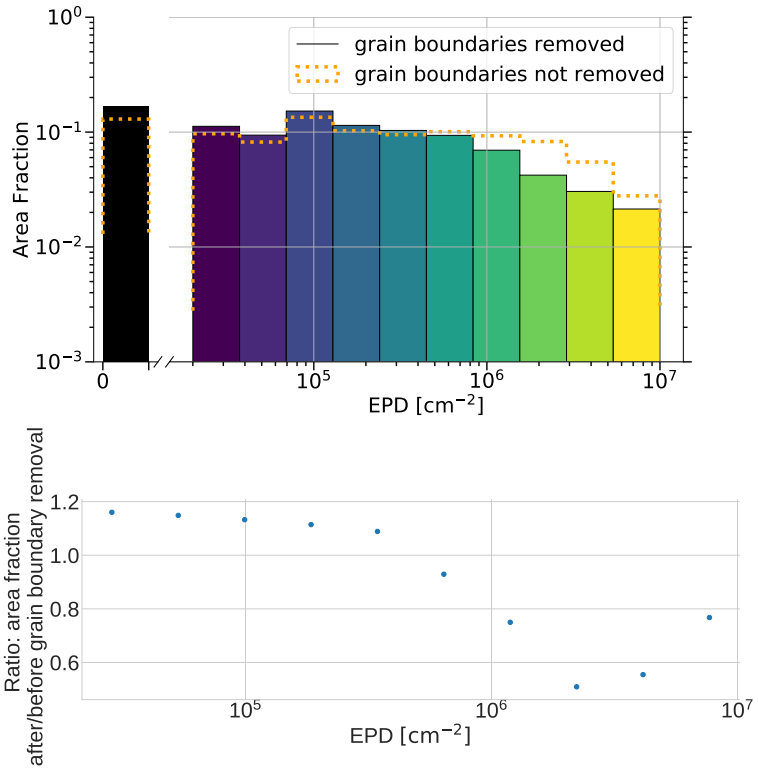

Figure 5: Top: an example of 1-d EPD histograms, calculated from the EPD data of figure 3, showing the area fraction of the wafer surface that is covered by a certain EPD. The histogram in solid colors shows the EPD after detection and removal of grain boundaries, while for the dotted histogram no distinction between grain boundaries and etch pit clusters has been made. Therefore, the dotted histogram does not represent the true EPD of the wafer. Bottom: the ratio of the above histograms.

6.1. Interpretation of EPD maps, limitations of the algorithm

In summary, when interpreting these EPD maps, the following points should be kept in mind:

- There is an upper limit to the EPD that can be detected with the optical microscope. This limit corresponds to an EPD of about $1 \times 10^7\,\mathrm{cm}^{-2}$. Cluster regions can exhibit much larger EPD values on highly localized sub regions, where EPD values of up to $2 \times 10^8\,\mathrm{cm}^{-2}$ could be measured.

- The lowest possible, non-zero EPD value, using a bin size b, is $\frac{1}{b}$. Figure 5 uses square bins with a side length of 62.5 µm, corresponding to a minimum EPD of $2.56 \times 10^4\,\mathrm{cm}^{-2}$.

- The number of etch pits in an etch pit conglomerate and the number of etch pits in a cluster are explicitly depending on the median etch pit size A. The value of A has been determined

from a set of identically etched wafers. A fixed value of $A = 18$ pixels, with a pixel size of 698 nm, is used here.

7. Conclusions

An automatic method for detection, density analysis and plotting of microscopic etch pit data of mc-Si material has been developed and the source code released as free and open source software. Grain boundaries and polishing scratches are identified and do not contribute to the etch pit density results. Etch pit data in low density regions is measured with high precision by detection of individual etch pits. Measuring etch pit data in mid density regions, where optical microscope images contain structures of multiple connected etch pits, requires assumptions about the expected etch pit size for computing EPD results. For high EPD regions of etch pit clusters, optical microscope data allows only for the calculation of a lower EPD limit that is based on the expected etch pit size. The published method is capable of analysing samples of several cm^2 on a regular office hardware in a few seconds and produces EPD results of unprecedented precision.

8. Acknowledgements

Part of this work was supported by the German Federal Ministry of Economic Affairs and Energy under contract nos. 0324041B and 0324001. The content is the responsibility of the authors.

9. Data Availability

The raw data and software code required to reproduce these findings are available to download from `https://data.mendeley.com/datasets/dv43z9x72t/1` .

References

[1] D. P. Fenning, A. S. Zuschlag, J. Hofstetter, A. Frey, M. I. Bertoni, G. Hahn, T. Buonassisi, Investigation of Lifetime-Limiting Defects After High-Temperature Phosphorus Diffusion in High-Iron-Content Multicrystalline Silicon, IEEE Journal of Photovoltaics 4 (3) (2014) 866–873. doi:10.1109/JPHOTOV.2014.2312485.

[2] H. J. Choi, M. I. Bertoni, J. Hofstetter, D. P. Fenning, D. M. Powell, S. Castellanos, T. Buonassisi, Dislocation Density Reduction During Impurity Gettering in Multicrystalline Silicon, IEEE Journal of Photovoltaics 3 (1) (2013) 189–198. doi:10.1109/JPHOTOV.2012.2219851.

[3] D. B. Needleman, H. Choi, D. M. Powell, T. Buonassisi, Rapid dislocation-density mapping of as-cut crystalline silicon wafers: Rapid dislocation-density mapping of as-cut crystalline silicon wafers, physica status solidi (RRL) - Rapid Research Letters 7 (12) (2013) 1041–1044. doi:10.1002/pssr.201308150.

[4] K. Adamczyk, G. Stokkan, M. Di Sabatino, Guidelines for establishing an etching procedure for dislocation density measurements on multicrystalline silicon samples, MethodsX 5 (2018) 1178–1186. doi:10.1016/j.mex.2018.09.013.

[5] M. Fleck, A. Zuschlag, G. Hahn, Etch Pit Density Reduction in POCl3 and Atmospheric Pressure Chemical Vapor Deposition-Gettered mc-Si, physica status solidi (a) 216 (17) (2019) 1900316. doi:10.1002/pssa.201900316.

[6] F. Secco d' Aragona, Dislocation Etch for (100) Planes in Silicon, Journal of The Electrochemical Society 119 (7) (1972) 948. doi:10.1149/1.2404374.

[7] D. G. Schimmel, Defect Etch for Silicon Evaluation (1979) 5.

[8] B. L. Sopori, A New Defect Etch for Polycrystalline Silicon, Journal of The Electrochemical Society 131 (3) (1984) 667. doi:10.1149/1.2115670.

[9] M. Wright Jenkins, A New Preferential Etch for Defects in Silicon Crystals, Journal of The Electrochemical Society 124 (5) (1977) 757. doi:10.1149/1.2133401.